ChemPubSoc Europe

DOI: 10.1002/chem.201405510

CHEMISTRY A European Journal Full Paper

Bioconjugates |Hot Paper|

Clickable 5′-γ-Ferrocenyl Adenosine Triphosphate Bioconjugates in Kinase-Catalyzed Phosphorylations

Nan Wang,[a, e] Zhe She,[a] Yen-Chun Lin,[a, b] Sanela Martić,[c] David J. Mann,[d] and Heinz-Bernhard Kraatz*[a, b]

A 5′-γ-ferrocenyl adenosine triphosphate (Fc-ATP) conjugate, Fc-CO-Lys-ATP, containing a clickable alkyne moiety was synthesized and compared to a non-alkynyl Fc-ATP analogue, Fc-CO-C6-ATP, as co-substrate in kinase-catalyzed phosphorylation reactions. Sarcoma-related kinase (Src), cyclin-dependent kinase (CDK2), and casein kinase II (CK2α) were chosen for this study. Surface electrochemical studies indicate that Fc-CO-Lys-ATP is an effective co-substrate due to the generated Fc current density signals, which is in line with the XPS measurement. Molecular modeling studies were also carried out to help understanding the high efficiency of Fc-CO-Lys-ATP as co-substrate in CDK2-catalyzed phosphorylation reactions. The steric hindrance due to Fc-CO-Lys-ATP binding to the Src active pocket, but not CDK2 kinase, negatively affects substrate interaction and reduces Fc-phosphorylation. The compatibility of Fc-CO-Lys-ATP with antiferrocene antibodies and a fluorescently labeled secondary antibody was also demonstrated in a biochemical format. Additionally, scanning electrochemical microscopy (SECM) was successfully used to probe the phosphorylation reaction for the first time. The clickable nature of Fc-CO-Lys-ATP was demonstrated on gold surfaces. The present study illustrates that Fc-CO-Lys-ATP is an efficient co-substrate for kinase-catalyzed phosphorylation reactions and adaptable to multiplex arrays.

Introduction

Protein kinases regulate the majority of cellular pathways through chemically adding phosphate groups, for example from an adenosine triphosphate (ATP) molecule, to other proteins, which accordingly results in modulation of downstream functions.[1] It has been shown that the over/under expression of certain protein kinases has been linked to human disease including many forms of cancer.[2] Consequently, assessing the activities and substrates of protein kinases is of great interest from a basic biological perspective and in terms of therapeutic targets.[1]

The traditionally used method for studying protein kinase activity is the [γ-^{32}P]ATP radiometric assay.[4] However, due to the well-known drawbacks of radioactive materials, environmental friendly methods are desired to replace this traditional approach. Thus, numerous techniques have emerged including electrochemical,[5] optical,[6] mass spectrometry,[7] and surface-plasmon resonance-based systems.[8] Among them, γ-phosphate-modified ATP analogues have been synthesized and demonstrated to be effective for these uses, such as biotin-, dansyl-, azide-, and ferrocene (Fc)-labeled ATP compounds.[9] Additionally, a systematic study of the compatibility between these ATP analogues and specific kinases (i.e., PKA, CK2, and Abl) has been reported recently.[10] Among the electrochemical systems, ferrocene-modified bioconjugates are one of the most widely used redox reporters due to their ideal electrochemical properties and their stability in aqueous solutions.[11] Numerous Fc–amino acid and Fc–peptide conjugates have been reported.[12] Their applications include but are not limit to peptide foldamers,[13] electrochemical detection,[14] and biomedical application.[15] In 2008, we reported the synthesis of a novel Fc-modified ATP conjugate, namely, 5′-γ-ferrocenyl-ATP (Fc-CO-C6-ATP), and the effectiveness of this compound as a co-substrate to detect the kinase-catalyzed phosphorylation reaction of surface-bound peptides (as shown in Scheme 1).[9d] Based on this discovery, a series of Fc-ATP derivative compounds have been synthesized and used for kinase activity and inhibitor screening studies.[16] These works provided valuable information for further understanding the exact nature of the interaction between the ATP co-substrate with the pep-

[a] Dr. N. Wang, Dr. Z. She, Y.-C. Lin, Prof. H.-B. Kraatz
Department of Physical and Environmental Science
University of Toronto Scarborough
1265 Military Trail, Toronto, Ontario M1C 1A4 (Canada)
E-mail: bernie.kraatz@utoronto.ca

[b] Y.-C. Lin, Prof. H.-B. Kraatz
Department of Chemistry, University of Toronto
80 St. George Street, Toronto, M5S 3H6 (Canada)

[c] Prof. S. Martić
Department of Chemistry, Oakland University
2200 North Squirrel Road
Rochester, Michigan 48309 (USA)

[d] Dr. D. J. Mann
Department of Life Sciences, Imperial College London
London SW7 2AZ (UK)

[e] Dr. N. Wang
Current address:
Beijing Key Laboratory of
Photoelectronic/Electrophotonic Conversion Materials
Department of Chemistry, Beijing Institute of Technology
Beijing 100081 (P.R. China)

Supporting information for this article is available on the WWW under http://dx.doi.org/10.1002/chem.201405510.

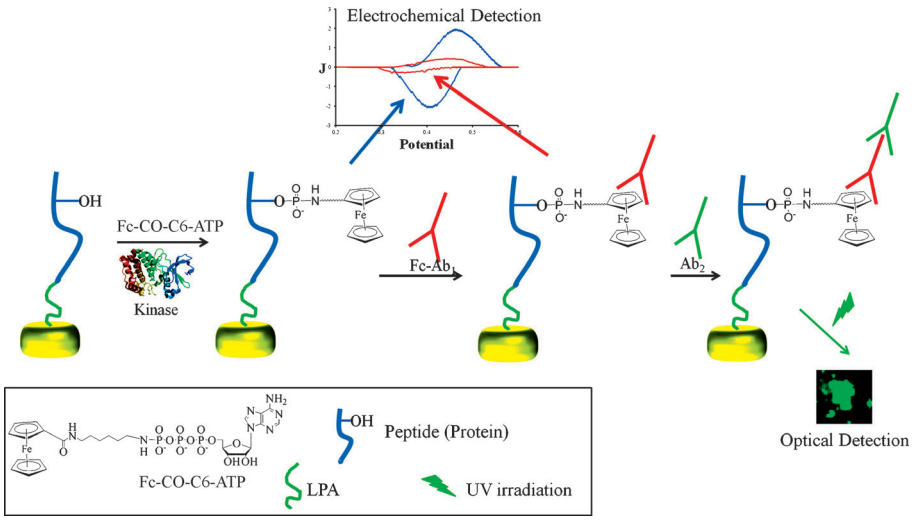

Scheme 1. Schematic illustration of the strategy and principle for the detection of kinase-catalyzed phosphorylation by using Fc-CO-C6-ATP and Fc-Ab_1/Ab_2. The peptide/protein (blue curve) is immobilized on the *N*-hydroxysuccinimide lipoic acid active ester (LPA) (green curve) modified Au surface. A protein kinase transfers the γ-phosphate-Fc group to the peptide, which is then further detected through electrochemical techniques. In an immunoassay approach, primary polyclonal antiferrocene antibodies (Fc-Ab_1) bind to the Fc-phosphates resulting in reduction of the electrochemical signals. This is followed by indirect immunodetection through fluorescently labeled goat anti-rabbit antibodies (Ab_2).

tide/proteins, as well as guidance for designing other effective Fc-ATP co-substrates.

In our recent study, we have also found that a robust polyclonal rabbit antiferrocene antibody (Fc-Ab_1) can selectively bind to Fc-modified bioconjugates in both solution and on surfaces.[17] By combining this bioanalytical tool with Fc-CO-C6-ATP, a powerful approach has been established, which can be applied to multiplex arrays and effectively monitor kinase activity by using both electrochemical and immunoassay detection methods as shown in Scheme 1.

In this work, we have designed and synthesized a novel Fc-ATP derivative, namely, Fc-CO-Lys-ATP, as shown in Scheme 2. Herein, the amino acid Lys(Boc)-OMe (Boc = *tert*-butoxycarbonyl) was used as a linker to connect the Fc moiety with the ATP functional group. The performance of this compound as a co-substrate in a kinase-catalyzed phosphorylation reaction was investigated with direct comparison to Fc-CO-C6-ATP as γ-phosphate donor. The extra alkyne moiety incorporated into Fc-CO-Lys-ATP allows further modification,[18] which has been demonstrated by successful attachment of an azide-labeled fluorescent dye through click chemistry. In addition, immunodetection and scanning electrochemical microscopy (SECM) were also used to detect a phosphotransfer involving this novel ATP derivative. This is the first time that SECM[19] has been used for monitoring phosphorylation process.

Results and Discussion

Synthesis and characterization of Fc-CO-Lys-ATP

The novel Fc-modified ATP compound was synthesized according to Scheme 2. The synthesis of the intermediate Fc-CO-Lys-Boc (**2**) was based on the employment of standard coupling methodology between an activated ester and Boc-protected alkyl amines in the presence of hydroxybenzotriazole, 1-ethyl-3-(3-dimethylaminopropyl)carbodiimide, and *N*,*N*-diisopropylethylamine.[12j] Fc-CO-Lys-Boc (**2**) was obtained with good yield (75%) and fully characterized by using NMR spectroscopy and mass spectrometry. The conversion of ATP into the γ-substituted derivate was achieved by following the literature procedure.[20] The Boc-protected conjugate Fc-CO-Lys-Boc was first deprotected in the presence of an excess of trifluoroacetic acid to generate the free amine **3**. Then the in-situ-formed adenosine metaphosphate was reacted with the free amine under

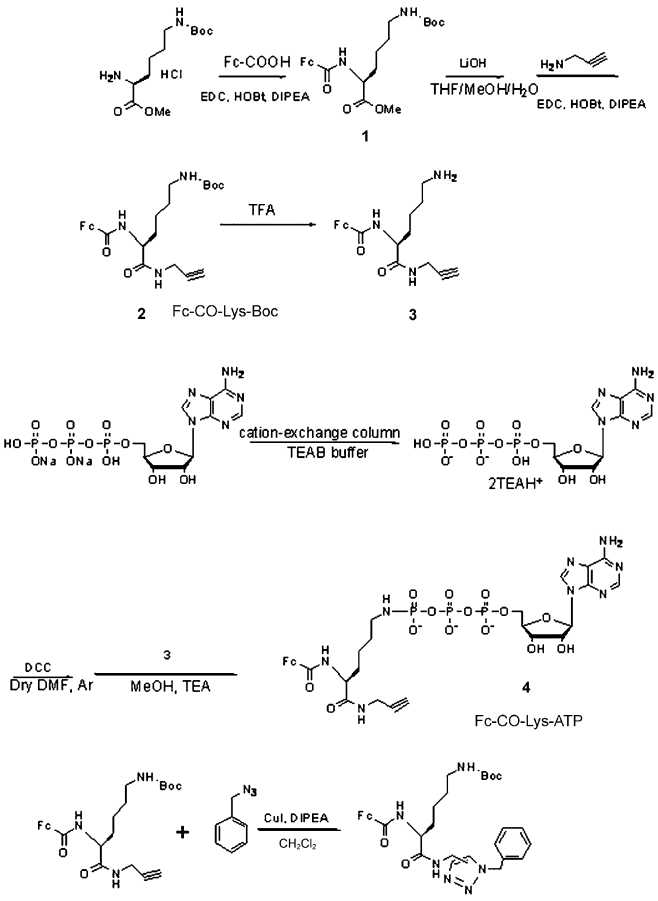

Scheme 2. Synthesis of Fc-CO-Lys-ATP and click reaction on Fc-CO-Lys-Boc. EDC = *N*′-(3-dimethylaminopropyl)-*N*-ethylcarbodiimide, HOBt = 1-hydroxybenzotriazole, DIPEA = diisopropylethylamine, TFA = trifluoroacetic acid, TEAB = tetraethylammonium bromide, DCC = dicyclohexylcarbodiimide, TEA = triethylamine.

Table 1. ^{31}P NMR chemical shifts and electrochemical data for the Fc conjugates.[a]

Fc compound	^{31}P NMR [ppm][b]	$E_{1/2}$ [mV]	ΔE [mV]	i_{pa}/i_{pc}	D[c]
Fc-CO-Lys-Boc	–	(574 ± 5)	(64 ± 5)	1.1	(22.1 ± 0.23)
Fc-CO-Lys-ATP	−0.96				
	−11.51	(434 ± 3)	(64 ± 8)	1.1	(3.06 ± 0.37)
	−23.01				
Fc-CO-C6-ATP	−0.78				
	−11.48	(431 ± 3)	(59 ± 8)	1.1	(4.54 ± 0.11)
	−22.98				

[a] Electrochemical data for compound Fc-CO-Lys-Boc was obtained at 0.1 mM in CH_3CN in the presence of 0.1 M TBAP. Data for compounds Fc-CO-Lys-ATP and Fc-CO-C6-ATP were measured at the concentration of 0.1 mM in the presence of 0.1 M $NaClO_4$ as the supporting electrolyte. Electrochemical data were measured by cyclic voltammetry with Ag/AgCl/3 M KCl as the reference electrode, a Pt wire as the auxiliary electrode, a glassy carbon surface as the working electrode. The scan rate was 100 mV s^{-1}. The reported error was obtained from the triplicate measurements. $E_{1/2}$ = half-wave potential; ΔE = peak separation; i_{pa}/i_{pc} = peak current ratio. [b] D_2O, 298 K, H_3PO_4 85% as an external NMR reference. [c] Diffusion coefficient is given in [× 10^{-5} cm^2 s^{-1}] and was determined electrochemically.

basic condition in the presence of DCC. After adding water, the byproduct was removed by precipitation and the solution was loaded onto a diethylaminoethyl (DEAE) cellulose column for further purification. The desired ATP coupling fractions were collected with 0.3–0.4 M TEAB (pH 7.5) and subjected to HPLC purification to give Fc-CO-Lys-ATP in 8% yield. Fc-CO-Lys-ATP was characterized by means of NMR spectroscopy and matrix-assisted laser desorption/ionization time-of-flight mass spectrometry (MALDI-TOF MS) (as shown in Figure S1 in the Supporting Information). In the ^{31}P NMR spectrum (as shown in Table 1), compound Fc-CO-Lys-ATP exhibited three signals coming from the α-, β-, and γ-P atoms, confirming the successful coupling of the ATP moiety. More importantly, the characteristic doublet peak for the γ-P atom at $\delta = -0.96$ ppm (vs. H_3PO_4) indicates the Fc-γ-phosphoamide formation.

In order to confirm that the alkyne moiety in this Fc derivative is clickable, a click reaction was carried out. Due to limiting amounts of Fc-CO-Lys-ATP, Fc-CO-Lys-Boc was used in a model reaction. Under typical copper(I)-catalyzed click reaction condition, Fc-CO-Lys-Boc reacted with benzyl azide successfully. The expected triazole derivative product was obtained with 82% yield. The synthesis and characterization details are given in the Supporting Information.

Electrochemistry of the Fc compounds in solution

The solution electrochemical properties of Fc-CO-Lys-Boc and Fc-CO-Lys-ATP were investigated by cyclic voltammetry (CV) in CH_3CN solution containing tetrabutylammonium perchlorate (TBAP) as electrolyte and in $NaClO_4$ solution, respectively. The data were summarized and are shown in Table 1. The data for Fc-CO-C6-ATP (the structure is shown in Scheme 1) was also included as a reference. All the Fc-modified compounds show a fully reversible one-electron wave with a peak separation (ΔE) in the range 50–80 mV versus Ag/AgCl. Fc-CO-Lys-Boc shows a half-wave potential ($E_{1/2}$) at approximately 574 mV and a peak current ratio (i_{pa}/i_{pc}) of 1.1, which is similar to other ferrocene compounds. Due to the solvent change (from CH_3CN to water)[16] Fc-CO-Lys-ATP and Fc-CO-C6-ATP show half-wave potential at approximately 430 mV. The diffusion coefficients (Ds) for all three compounds were also calculated by using the Randles–Sevcic equation,[21] which demonstrates the effect of different molecule sizes on their mobility and redox activity in solution. As expected, the ATP-free compound Fc-CO-Lys-Boc has a larger D value than the ATP-modified compounds.

Electrochemical, fluorescent, and XPS detections of protein kinase-catalyzed Fc phosphorylations

To investigate the general application of Fc-CO-Lys-ATP as a co-substrate in protein kinase-catalyzed phosphorylation reactions, three protein kinases, that is, Src, CDK2 in combination with cyclin A, and CK2α, were chosen as representative kinases that act on Tyr, Ser, or Thr residues for the following electrochemical studies. Src is a protein Tyr kinase that is over expressed in some forms of cancer.[22] CDK2 is mainly involved in the cell cycle and division and acts on Ser and Thr residues.[23] CK2α is primarily involved in the cellular metabolism and differentiation and acts on Ser/Thr residues in key regulatory proteins.[24] Fc-CO-C6-ATP, a demonstrated effective co-substrate, was employed as a control.

Cyclic voltammetry and square-wave voltammetry (SWV) were used for electrochemical studies of peptides bound to a gold surfaces in the presence of ferri/ferrocyanide ($[Fe(CN)_6]^{3-/4-}$) as a redox probe. As shown in Figure 1, the current density observed is reduced with each step of modification until the loss of the redox probe signal and the peak po-

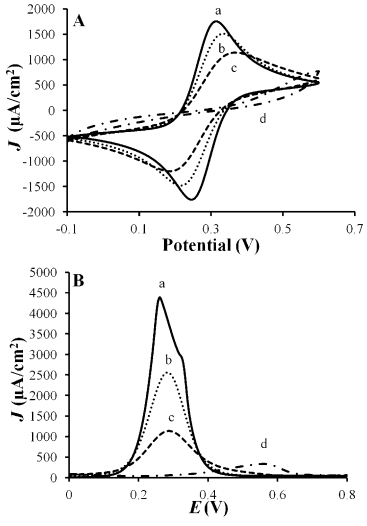

Figure 1. A) Cyclic voltammograms and B) square-wave voltammograms for peptide-modified gold electrodes in a 1 M $NaClO_4$ solution containing 5 mM of the $[Fe(CN)_6]^{3-/4-}$ redox probe: a) bare gold electrode, b) after modification with LPA, c) after immobilization of the peptide substrate, and d) after blocking with 100 mM ethanolamine and following with 10 mM dodecanethiol. Ag/AgCl/3 M KCl mixture was used as reference electrode, a Pt was included as auxiliary electrode. The scan rate was 100 mV s^{-1}.

tential in the SWV (Figure 1B) shifts from approximately 0.26 V to about 0.58 V. The results indicate a lower electron-transfer ability through the surface due to blockage of growing films with the corresponding peptides and blocking reagent.

Next, the kinase-catalyzed Fc phosphorylation was carried out by using these peptide-modified gold electrodes, Fc-ATP analogues, and their corresponding kinases in the presence of kinase assay buffers. CVs and SWVs were recorded after the reaction. The representative CVs and SWVs for Src-catalyzed reactions are given in Figure 2. The CV data show that Fc-CO-C6- and Fc-CO-Lys-phosphorylated peptide films display very similar formal redox potential, E^{o}, located at approximately 490 mV due to the similar structure of the Fc-CO-C6- and Fc-CO-Lys moiety, and also indicate the presence of redox-active Fc groups on the surface. Because the protein kinases transfer the Fc phosphate groups provided by the Fc-ATP analogues in this phosphorylation process to the peptide substrates, the Fc labels on the surface can be electrochemically evaluated and

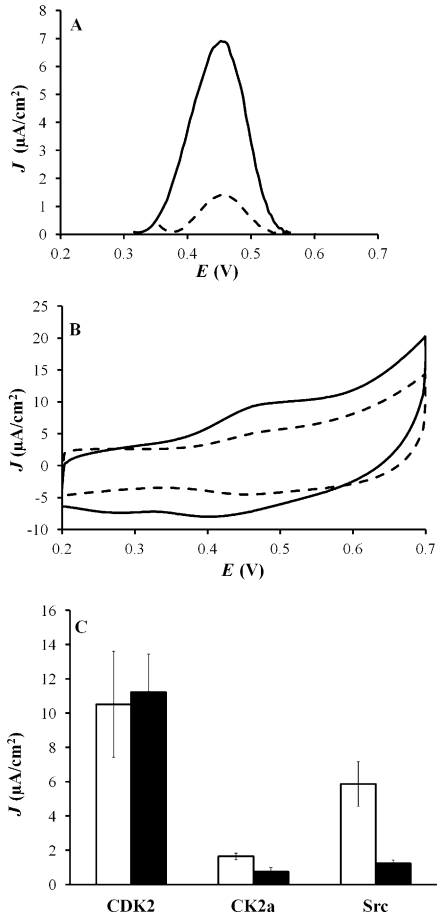

Figure 2. A) Square-wave voltammograms and B) cyclic voltammograms showing the current densities of modified surfaces following the Src kinase-catalyzed phosphorylation reaction in the presence of compounds Fc-CO-Lys-ATP (dashed lines) and Fc-CO-C6-ATP (solid lines). C) Plot of the current densities of surfaces following the phosphorylation reactions with CDK2, CK2α, and Src in the presence of Fc-CO-Lys-ATP (black bars) and Fc-CO-C6-ATP (white bars). Data points are the average of at least triplicate measurements taken from SWVs. Measurements were taken in 1 M $NaClO_4$ aqueous solution with Ag/AgCl/3 M KCl as the reference electrode, a Pt wire as the auxiliary electrode, and a scan rate of 100 mV s^{-1}.

the magnitude of the redox signal of Fc is directly related to the efficiency of the co-substrate. Consequently, Fc-CO-C6-ATP is a better co-substrate than Fc-CO-Lys-ATP, due to the higher redox signals observed in SWV as shown in Figure 2A.

In order to confirm that the current signal was generated from the surface-attached Fc moiety rather than diffusive contributions, CV measurements with different scan rates were also applied. As shown in the Supporting Information (Figure S7), the linear dependence of the anodic and cathodic current density versus the scan rate clearly illustrates the existence of surface chemically attached Fc groups.

Besides Src kinase, similar CV and SWV results were also obtained by using CDK2 and CK2α, however, Fc-CO-C6-ATP did not always perform better than Fc-CO-Lys-ATP as co-substrate. The electrochemical results given in Figure 2C indicate that Fc-CO-C6-ATP displays better performance in the case of Src and CK2α, because greater current densities were observed, whereas in the case of CDK2 nearly equal current densities were obtained by using these two co-substrates. In general, the different efficiencies between the Fc-ATP analogues in the kinase-catalyzed phosphorylation reactions might be explained by steric hindrance and electronic factors.[16] Our previous work has demonstrated that a long alkyl spacer with more than six carbon atoms can effectively reduce the steric hindrance and hence help to maintain the kinase activity with Src.[16a] Moreover, in order to be a good co-substrate, additional hydrogen-bonding and electrostatic interactions should be avoided.[16b] In this work, comparing the linker in Fc-CO-Lys-ATP with the one in Fc-CO-C6-ATP, the lysine moiety is only one carbon atom short, but the existence of an amide-linked alkyne moiety possibly introduces extra conformational constraints with respect to the active sites of the protein kinase. Furthermore, even though the alkyne moiety in Fc-CO-Lys-ATP has a low polarity as other hydrocarbon functional groups,[25] the amide group that linked the ferrocenyl and alkyne groups together still brings in additional hydrogen-bonding and electrostatic interactions with the catalytic pocket of the kinase or the incoming peptide substrate. As a result, the extra amide group negatively affects the phosphoryl transfer process.

In our previous work, we found that with Src and CK2α the current density generated by the resulting phosphorylated Fc peptides significantly decreased with an increasing length and polarity of the linker, whereas with CDK2 the current density increased.[16b] Based on this observation it is likely that the influence of electronic factors is less pronounced with CDK2 than with Src and CK2α.

To further confirm the formation of the Fc-CO-Lys-phosphopeptide through a kinase-catalyzed phosphorylation reaction by using Fc-CO-Lys-ATP as co-substrate, XPS was used to prove the existence of Fc on the surface. The XPS survey scans of the peptide film after phosphorylation in the presence of CDK2 is provided in the Supporting Information (Figure S8); these reveal the presence of S, C, and N elements in the films. The XPS spectrum obtained with fifty scans given in Figure S9 in the Supporting Information shows that a peak at 711.9 eV was observed only when kinase was used. The binding energy of this peak indicates the presence of Fe $2p_{3/2}$ on the surface,

which resulted from a Fc-labeled phosphoryl transfer and this observation is in good agreement with previous works.[26] In the control experiment, when Fc-CO-Lys-ATP was present and CDK2 kinase was absent, no corresponding signals related to the Fc group were observed as shown in Figure S9 in the Supporting Information (dashed line).

We also tested the compatibility of Fc-CO-Lys-ATP with the antiferrocene antibody and fluorescently labeled secondary antibody for monitoring protein kinase activity on a surface. Initially, the electrochemical method was applied to detect the performance of the Fc-Ab_1 in the CDK2-catalyzed phosphorylation reaction. As shown in Figure S10 in the Supporting Information and Figure 3A, after incubation with Fc-Ab_1 at 1:500 dilution, the current signals decreased from approximately 2 and 0.5 $\mu A\,cm^{-2}$ down to 0.4 and 0.1 $\mu A\,cm^{-2}$ for Fc-CO-C6-phosphopeptide and Fc-CO-Lys-phosphopeptide films, respectively, due to the binding of Fc-Ab_1 to the Fc groups on the surface. This dramatic electrochemical signal-off response indicates that compared to the C_6 linker, the modified lysine linker does not greatly interfere with the recognition between the Fc group and the antiferrocene antibody, confirming the compatibility and usefulness of Fc-CO-Lys-ATP in this detection strategy.

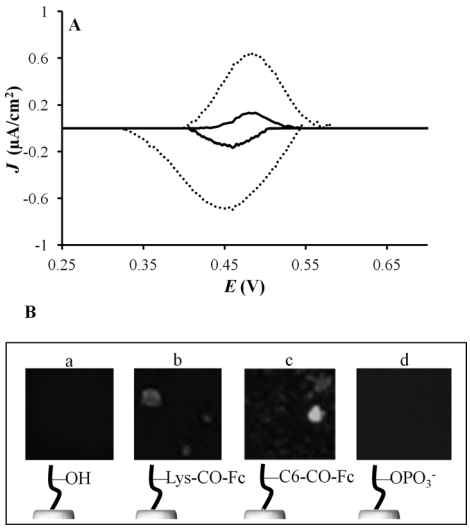

Figure 3. A) Immuno-electrochemical detection of Fc phosphorylation of immobilized peptides. Background-subtracted cyclic voltammograms of the Au surfaces containing the Fc-CO-Lys-ATP-phosphorylated CDK2 substrate peptide films before (dash lines) and after (solid lines) addition of Fc-Ab_1 (1:500). B) Fluorescence images of a) peptide-modified, b) Fc-CO-Lys-phosphopeptide-modified, c) Fc-CO-C6-phosphopeptide-modified, and d) phosphopeptide-modified Au surfaces following the addition of Fc-Ab_1 (1:500) and fluorescent Ab_2 (1:100). Filter set 17 was used to generate the images. Colored images are given in the Supporting Information.

An indirect fluorescence imaging study was also carried out by using antiferrocene antibodies to visualize the phosphorylated peptide films by using different ATP substrates. In this study, a CDK2-catalyzed phosphorylation reaction was performed on a peptide-modified Au surface in the presence of Fc-CO-Lys-ATP, Fc-CO-C6-ATP, and unmodified ATP co-substrates. The unphosphorylated peptide film was included as a control. The fluorescence images (Figure 3B) indicated that reactions using Fc-CO-C6-ATP and Fc-CO-Lys-ATP generated visible fluorescence under irradiation, confirming the effectiveness of Fc-CO-Lys-ATP in the phosphorylation reaction and the compatibility of the Fc-CO-Lys fragment with the immunodetection system. As expected, the antiferrocene antibodies did not bind to either the peptide or the phosphopeptide films (treated with unmodified ATP), these samples demonstrating background fluorescence only (Figures 3Ba) and d)).

Molecular modeling studies

To rationalize the different efficiency between Fc-CO-Lys-ATP and Fc-CO-C6-ATP as co-substrate in kinase-catalyzed phosphorylation reactions, we modeled both ATP derivatives into the active site of Src and CDK2/cyclin A. With the Src kinase (PDB 1y57), the Fc groups in both Fc-ATP compounds were well outside the ATP binding pocket and exposed to the solvent as shown in Figure 4A, making them theoretically tolerable. However, the additional alkyne group of Fc-CO-Lys-ATP introduced potential steric hindrance between the acetylene proton and the surrounding Src amino acids (Figure 4C). This observation may explain the higher catalytic activity for Src with un-functional Fc-CO-C6-ATP than with Fc-CO-Lys-ATP because the latter substrate induced steric hindrance at the binding pocket of the kinase.

Modeling of both Fc-ATP analogous into the CDK2/cyclin A ATP binding site (PDB 4eoo) resulted in favorable overall binding modes. As shown in Figure 5A both compounds may protrude into the cyclin A binding interface to the CDK2 protein, but may not negatively affect the CDK2/cyclin A complexation. The distance between the acetylene proton to the surrounding amino acids is around 2 Å as shown in Figure 5C, indicating the more significant steric hindrance between Fc-CO-Lys-ATP and the active site. However, with CDK2, both Fc-ATP compounds display similar efficiency. To explain this, the peptide substrate binding should also be taken into account. Considering the CDK2 residues that bind the peptide substrate,[27] only 50Arg is close to the Fc group but not to the alkyne moiety as shown in Figure 5B. Due to peptide substrate binding away from the Fc side, the substitution of Fc-ATP would not appear to significantly influence the final phosphoryl transfer outcome. In contrast, with Src the residues that bind the peptide substrate are 343–519.[28] Among these, residues 384–402 are critical. As shown in Figure 4B all residues surrounding the alkyne moiety belong to this list of amino acids. As a result, the introduction of this functional group may influence the phosphorylation reaction more substantially. It is also noteworthy that all the above-described molecular modeling studies are based on the native state, whereas our electrochemical study is carried out on a surface with the environment of the substrate known to influence the phosphoryl transfer process.[10]

Scanning electrochemical microscopy (SECM)

As a complimentary method to the above-described electrochemical and optical investigations, SECM was used to investi-

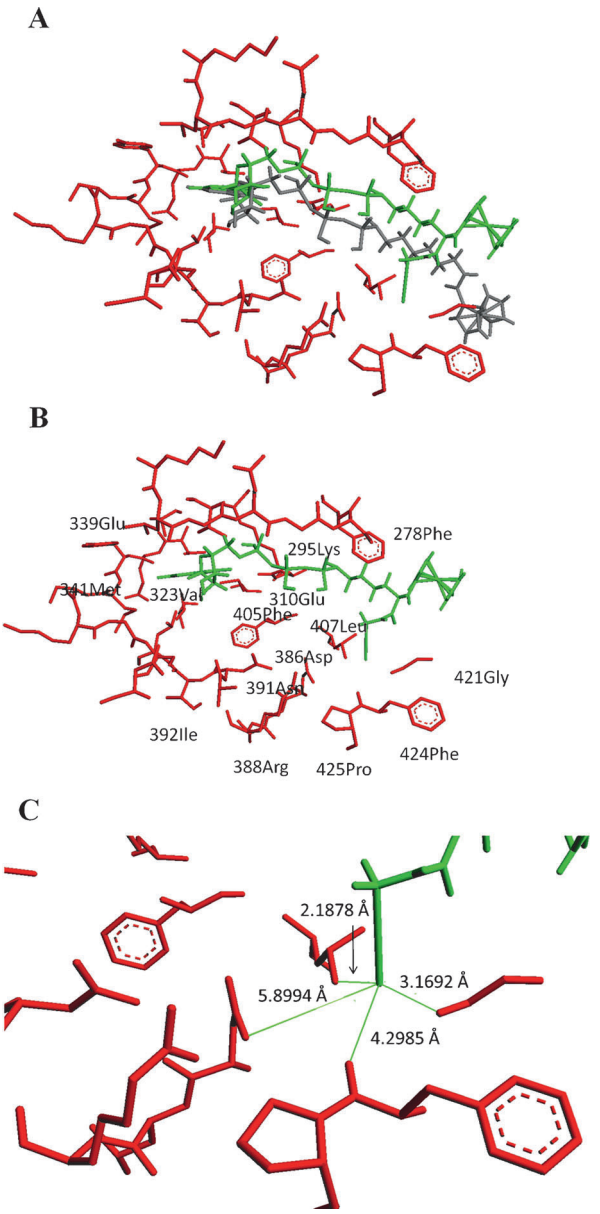

Figure 4. A) Molecular modeling of Fc-CO-Lys-ATP and Fc-CO-C6-ATP into the active site of Src. B) Molecular modeling of Fc-CO-Lys-ATP into the active site of Src showing key amino acids. C) Proximity of the acetylene proton to surrounding amino acids of Src. Colored images are given in the Supporting Information.

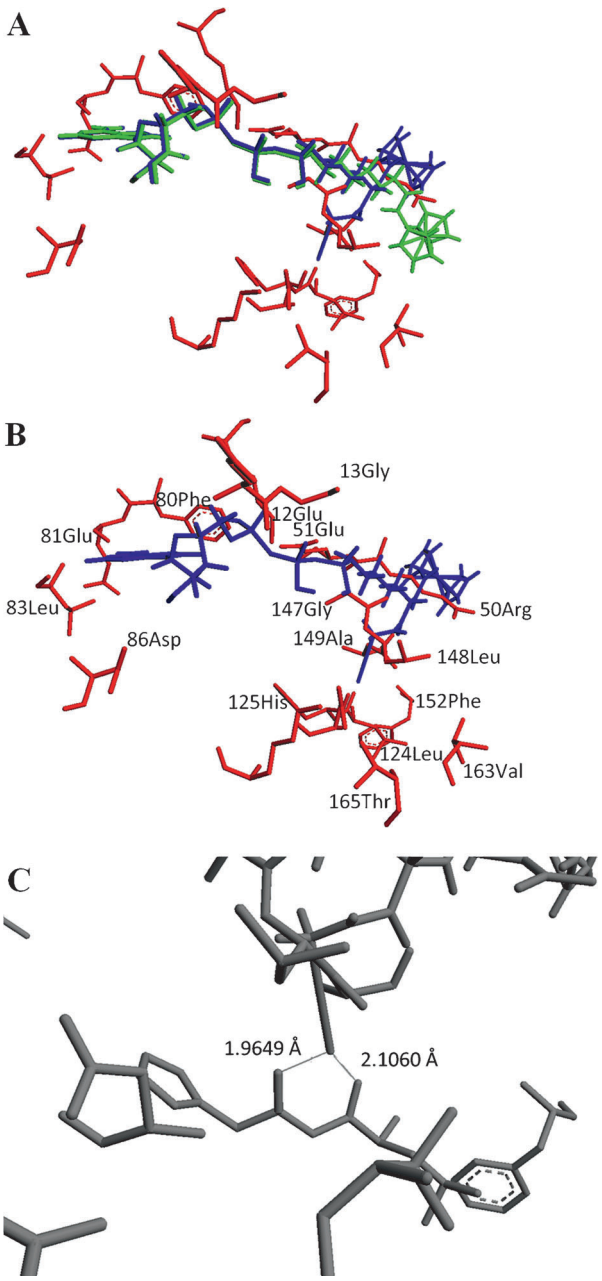

Figure 5. A) Molecular modeling of Fc-CO-Lys-ATP and Fc-CO-C6-ATP into the active site of CDK2. B) Molecular modeling of Fc-CO-Lys-ATP into the active site of CDK2 showing the key amino acids. C) Proximity of the acetylene proton to surrounding amino acids of CDK2. Colored images are given in the Supporting Information.

gate the peptide films before and after the CDK2 kinase-catalyzed phosphorylation reaction. To the best of our knowledge, this is the first time that SECM has been used to monitor phosphorylation reactions. Instead of using a gold or gold-modified electrode with a large surface area (several square millimeters), a Pt microelectrode was employed for evaluating the electrochemical properties of the surfaces at smaller scale of approximately hundreds of square micrometers. The working principle of SECM has been well discussed before.[19d, 29]

The electrochemical property of the surface was dramatically changed when the bare gold surface was modified with LPA self-assembled monolayers (SAMs). A negative feedback was observed for LPA SAMs, as shown in Figure 6. The current decreased during the approach of the tip to the substrate. This is expected, as the SAMs on the gold surface will be more insulating and the layer minimizes the electron charge transfer between the gold substrate and the redox probe, thus the regeneration of Fe^{2+} from Fe^{3+} by the substrate is compromised and obstruction of the Fe^{2+} diffusion dominates the process.[29a,b] The electron charge-transfer process was further reduced by immobilization of the CDK2 peptide onto LPA. The SECM data in Figure 6 show that the steady current observed during the approach was even less for the surface after CDK2 peptide binding than before. The additional insulating layer of

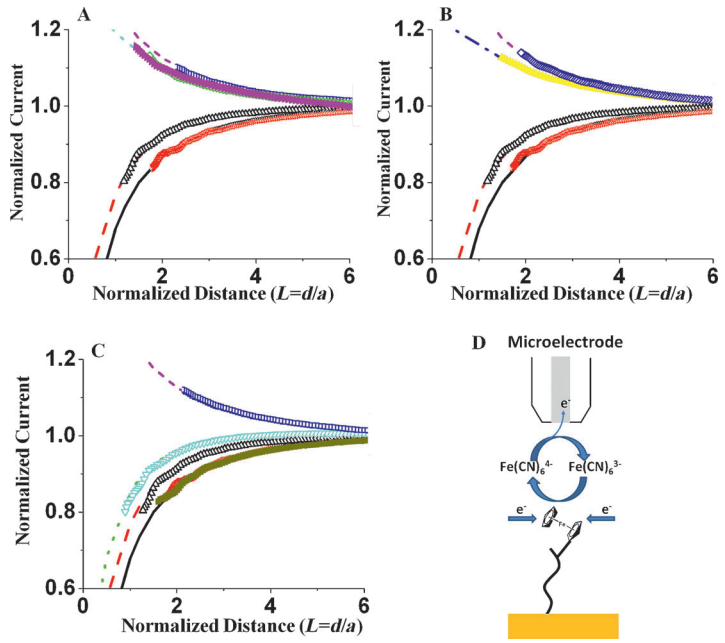

Figure 6. Examples of SECM approach curves obtained for three sets of samples using different co-substrates: A) ATP, B) Fc-CO-C6-ATP, and C) Fc-CO-Lys-ATP. Approach curves for the following surfaces are presented in the figure: bare gold (□); gold modified with LPA (△), immobilized CDK2 peptides after blocking by 100 mM ethanolamine and following with 10 mM dodecanethiol. After phosphorylation by using ATP in the presence of CDK2 kinase (◇) and followed by exposure to Fc-Ab_1 (▶). After phosphorylation by using Fc-CO-C6-ATP in the presence of CDK2 kinase (○) and followed by exposure to Fc-Ab_1 (▲). After phosphorylation by using Fc-CO-Lys-ATP in the presence of CDK2 kinase (▽) and followed by exposure to Fc-Ab_1 (■). The continuous and dashed lines are the approach curves calculated by COMSOL Multiphysics simulation[19b,c] by using known values of dimensionless rate constants (Λ). The tip steady-state current was normalized against the current determined at an infinite distance from the substrate. The normalized distance (*L*) is the ratio of tip/substrate separation (*d*) to the tip radius (*a*). D) Illustration of SECM measurements: positive feedback generated from catalytic oxidation of $[Fe(CN)_6]^{4-}$ over ferrocenyl peptide.

peptide increases the film thickness, which makes the electron transfer channels even longer. Three sets of phosphorylation experiments were carried out on the peptide-immobilized surfaces by using unmodified ATP, Fc-CO-C6-ATP, and Fc-CO-Lys-ATP as co-substrates under identical conditions and their corresponding approach curves have been obtained as shown in Figures 6A–C. By using unmodified ATP as co-substrate, a positive feedback was observed as shown in Figure 6A. It is likely due to the reason that the CDK2 peptide, HHASPRK, has multiple free amine groups (His, Arg, and Lys) that can react with the LPA SAMs, resulting in a more closely packed neutral peptide film. After introducing the negatively charged phosphate groups into the Ser residue through kinase-catalyzed phosphorylation, defects in the film were created due to ionic repulsion interaction. Thus, there would be more channels for electron charge transfer and the current would increase as the tip approaches the substrate. This hypothesis is in agreement with the CV and impedance measurements. As shown in Figures 7A and B, after phosphorylation, the current signal is recovered and the film resistance decreased.

Figure 6B illustrates that the positive feedback was also observed for Fc-phosphorylated peptide film by using Fc-CO-C6-ATP as co-substrate. In this case, Fc groups were attached onto the peptide surface through phosphoryl transfer reactions.[9d] The Fc layer seemed to have a similar conductive ability to metal surfaces and could efficiently distribute the charges, as shown in Figure 6D, and promote the regeneration process, which is consistent with other similar Fc monolayer systems.[30] However, negative feedback was observed for the Fc-CO-Lys-phosphopeptide as shown in Figure 6C. In this case, although the charge-transfer property of the Fc-CO-Lys-phosphopeptide film was less efficient than of the Fc-CO-C6-phosphopeptide film (positive feedback), the charge-transfer property of this film was still improved by the introduced Fc groups compared to the unmodified peptide film.

The antiferrocene antibody was also used in the SECM studies to probe the existence of Fc on the sample surfaces. The unmodified ATP-treated peptide surface showed no changes before and after antibody treatment indicating no non-specific effects (Figure 6A). When Fc-Ab_1 was applied to surfaces treated with Fc-CO-C6-ATP and Fc-CO-Lys-ATP, respectively, the approach curves shown in Figures 6B and C were seen to have a reduced steady-state current, which is consistent with antibody immobilization. In order to evaluate the result more quantitatively, simulation of approach curves with a known surface regeneration rate was conducted following a published procedure[19c,31] and by using the COMSOL Multiphysics software.[19b,c] The experimental curves were compared with the simulated ones to estimate the regeneration kinetics.

The rate constants plot in Figure 8 shows that the unmodified gold surface had the highest regeneration rate of Fe^{3+} to Fe^{2+} at $(1.55\pm0.29)\times10^{-3}$ cm s^{-1}. The rate dropped dramatically to $(7.63\pm2.41)\times10^{-5}$ cm s^{-1} when the gold was modified with LPA. A further decrease was seen after immobilization of the CDK2 peptide and the regeneration rate was decreased to $(5.47\pm2.94)\times10^{-5}$ cm s^{-1}. Phosphorylation of the immobilized peptide with unmodified ATP, Fc-CO-C6-ATP, and Fc-CO-Lys-ATP by CDK2 kinase, respectively, increased the regeneration rates to $(9.95\pm1.62)\times10^{-4}$, $(1.39\pm0.28)\times10^{-3}$, and $(1.83\pm0.06)\times10^{-4}$ cm s^{-1}, respectively. The regeneration rates for the Fc-CO-C6-phosphopeptide surfaces were the fastest of all the treated samples and were approximately 10% slower than the bare gold. As discussed in the description for Figure 6, phosphorylation with ATP possibly creates defects for electron charge transfer, Fc groups transferred to the peptide surfaces might also be able to promote the regeneration process by reduction and oxidation of their Fe centers. The Fc-CO-Lys-phosphopeptide surfaces had the lowest regeneration rates. This is possibly due to the steric hindrance produced by having a lysine group in the chain, thus the regeneration rates for Fc-CO-Lys-phosphopeptide surfaces would rely mostly on the Fc group only. The regeneration rates for phosphate-peptide surfaces were not changed by the treatment with the anti-

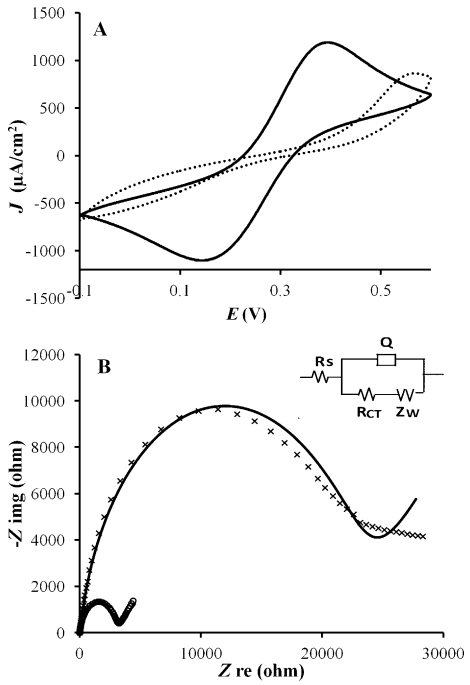

Figure 7. Surface characterization of the CDK2 peptide film in a 1 M $NaClO_4$ solution containing 5 mM $[Fe(CN)_6]^{3-}/^{4-}$ as redox probe. A) Cyclic voltammograms and B) Nyquist plots before (dashed lines or ×) and after (solid lines or ○) phosphorylation reaction by using CDK2 kinase with Fc-CO-C6-ATP. Ag/AgCl was used as the reference electrode, a Pt wire was used as auxiliary electrode, a scan rate of 100 mV s^{-1} was used. The impedance spectra were recorded in the frequency range of 100 kHz to 0.1 Hz with a AC amplitude of 5 mV. Experimental data are shown as points and calculated results correspond to solid lines. The inset shows the equivalent circuit model: R_S is the solution resistance, Q is the constant phase elements, R_{CT} is the charge-transfer resistance, and Z_W is the finite length Warburg impedance.

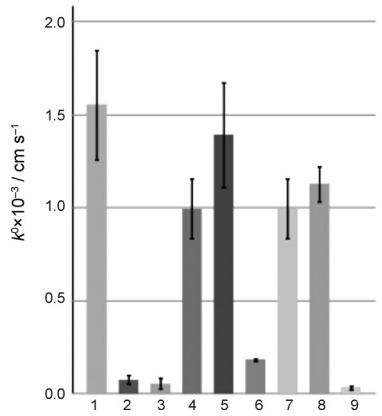

Figure 8. Rate constant, k^0, plots for the surfaces indicated in the figure. These rate constants were measured by using the Λ values estimated by the comparison of the experimental approach curves against the calculated approach curves from COMSOL Multiphysics simulations, both examples of which are shown in the Figure 6. No. 1: bare gold, 2: LPA, 3: peptide film, 4: phosphate-peptide, 5: Fc-CO-C6-phosphopeptide, 6: Fc-CO-Lys-phosphopeptide, 7: phosphate-peptide+antibody, 8: Fc-CO-C6-phosphopeptide+antibody, 9: Fc-CO-Lys-phosphopeptide+antibody.

ferrocene antibody, as shown in Figure 8, No. 4 and 7. This is consistent with the examples discussed earlier for the approach curves shown in the Figure 6. The regeneration rates for Fc-CO-C6-phosphopeptide and Fc-CO-Lys-phosphopeptide surfaces decreased to $(1.13 \pm 0.09) \times 10^{-3}$ and $(3.32 \pm 0.94) \times 10^{-5}$ cm s^{-1}, respectively, after the binding by the antibody, because the electron transfer between Fc and the redox probe is blocked by the attachment of non-conductive Fc-Ab_1. SECM investigation not only provides a complementary method to electrochemical characterizations, but it is also a method to monitor the electrochemical property at more localized sample areas.

Click reaction on Fc-CO-Lys-phosphopeptide films

The extra alkyne moiety incorporated into the Fc-CO-Lys-ATP compounds allows further modification. To further determine the utility of this functionalized ATP compound, a surface-based click reaction was designed as shown in Figure 9. In this reaction, CK2α peptide was first immobilized onto the Au surface and then phosphorylated by using CK2α kinase with Fc-CO-Lys-ATP as co-substrate. The phosphorylated film further reacted with Azide-fluor 488 through a click reaction catalyzed by Cu^I. In this study, Fc-CO-C6-ATP, the un-functionalized Fc-ATP compound, was also included as a control. The fluorescence images were collected as shown in Figure 9. The image in entry 1 clearly shows that the film formed by using Fc-CO-

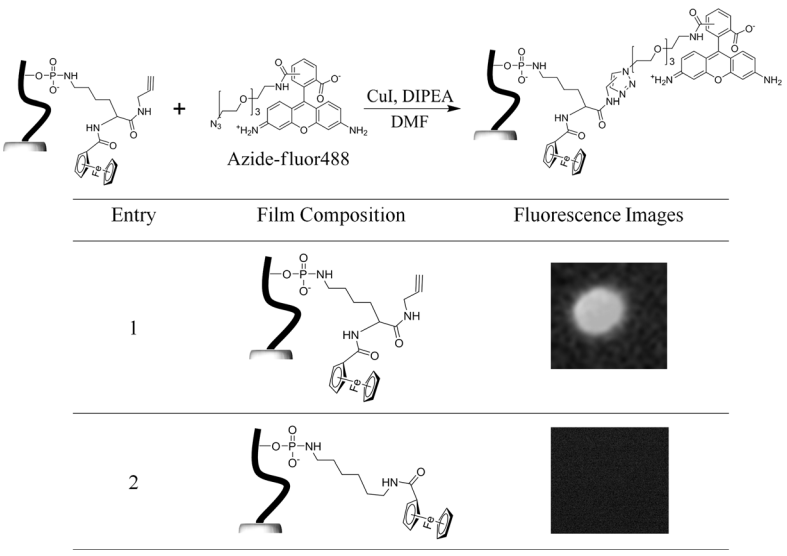

Figure 9. Fluorescence images of 1) Fc-CO-Lys-phosphopeptide-modified and 2) Fc-CO-C6-phosphopeptide-modified Au surfaces after a Cu^I-catalyzed click reaction with Azide-fluor488. Colored images are given in the Supporting Information.

Lys-ATP generated visible fluorescence under irradiation, confirming the attachment of the fluorescent fluor488 fragment. Due to the lack of an alkyne moiety, the Fc-CO-C6-phosphopeptide displayed only weak background fluorescence signals as shown in entry 2.

Conclusion

A new Fc-ATP compound containing a functional alkyne moiety has been synthesized and characterized. A comparative electrochemical study between this compound and related Fc-CO-C6-ATP was carried out by using surface-bounded peptides phosphorylated by Src, CDK2, and CK2α kinases. Obvious electrochemical signals were detected, indicating the effectiveness of Fc-CO-Lys-ATP as co-substrate in the reaction. These studies also show that this compound can be applied to the Fc-Ab_1/Ab_2 system, providing both electrochemical results and immunodetection. An azide-attached organic dye was successfully linked to this Fc-CO-Lys-phosphate peptide film through click chemistry. Thus, this compound has significant potential for further application in the study of enzymatic post-translations and we will evaluate the feasibility of "clickable" substrates to replace the well-established immunoassay.

Experimental Section

General methods

All synthesis reactions were carried out under air unless indicated otherwise. *N*,*N*-Diisopropylethylamine, propargylamine, diethylaminoethyl cellulose, adenosine 5′-triphosphate disodium salt, Azide-fluor488, and *N*,*N*′-dicyclohexylcarbodiimide were obtained from Sigma Aldrich and used as received. Dowex AG 50W-X8 was purchased from Bio-Rad Laboratories (Ontario, Canada). H-Lys(Boc)-OMe·HCl, hydroxybenzotriazole, and 1-ethyl-3-(3-dimethylaminopropyl)carbodiimide were bought from AAPPTec LLC (KY, USA). Dry dimethylformamide was purchased from Fisher Scientific. Dichloromethane was distilled by using CaH_2 before use. Methanol was distilled from magnesium turnings with the presence of iodine. Ferrocenecarboxylic acid,[32] Fc-CO-Lys(OMe)-NHBoc (**1**),[33] and adenosine 5′-[γ-ferrocene] triphosphate (Fc-CO-C6-ATP)[9d] were prepared according to the literature procedures assigned to each compound. ^{1}H and ^{31}P NMR experiments were performed on a Bruker Advance 500 MHz spectrometer. The initial geometry of Fc-CO-C6-ATP and Fc-CO-Lys-ATP conjugates was energy-optimized by Gaussian.[34] The optimized co-substrate structures were superimposed onto the binding site of the Src kinase (PBD 1y57) and CDK2/Cyclin A kinase (PBD4eoo) and modeled by ArgusLab 4.0.1 (Mark A. Thompson, Planaria Software LLC, Seattle, WA, USA, http://www.arguslab.com).

The Src peptide substrate, EGIYDVP, was obtained from BioBasic Inc (Markham, Ontario). The CDK2 peptide substrate (HHASPRK), the CDK2/cyclin A complex, and the Src kinase were purchased from Cell Signaling (New England Biolabs Ltd., Pickering, Ontario). The CK2α and the peptide substrate (RRRDDDSDDD) were prepared in the laboratory of D. W. Litchfield (University of Western Ontario).

Serum enriched with polyclonal rabbit antiferrocene antibodies (Fc-Ab_1) was produced at the YenZym Antibodies, LLC (CA, U.S.) against the monosubstituted ferroceneamide-alkylamine and used without further purification. Goat anti-rabbit IgG (H + L) secondary antibody, DyLight 488 conjugate was purchased from Thermo Scientific, Canada.

Synthesis

Preparation of Fc-CO-Lys-Boc (2): Compound **1** (400 mg) was dissolved in MeOH/H_2O/THF (3 mL:3 mL:1 mL). Then LiOH (6 equiv) was added to this solution. The reaction mixture was stirred in the dark at RT for two days. Then THF was removed in vacuum and water (15 mL) was added. The aqueous phase was washed with dichloromethane (3×10 mL) and then treated with 2 M HCl till pH ≈2 was reached. Dichloromethane (15 mL) was added to dissolve the precipitate, which was further washed with brine (3×10 mL) and dried over $MgSO_4$. After solvent removal, the yellow solid (Fc-CO-Lys(OH)-NHBoc) was used in the next step without further purification. EDC·HCl (1.38 mmol, 266 mg, 2.5 equiv) and HOBt (1.38 mmol, 213 mg, 2.5 equiv) were added to an anhydrous solution of Fc-CO-Lys(OH)-NHBoc (250 mg, 1 equiv) in dichloromethane (15 mL) on an ice bath. Then DIPEA (0.14 mL, 2.5 equiv) and propargylamine (1.1 mmol, 61 mg, 2 equiv) were added to this solution. The reaction mixture was continuously stirred overnight under N_2 atmosphere. After the reaction was completed, the solution was washed with saturated aqueous $NaHCO_3$ solution (3×50 mL), 10% critic acid (3×50 mL), and brine (3×50 mL). The organic layers were dried over $MgSO_4$ and the solvent was evaporated. The residues were purified by column with dichloromethane/MeOH (97:3) to isolate the product as yellow solids (yield 75%). ^{1}H NMR (DMSO, 298 K): δ = 8.32 (t, J = 5.0 Hz, 1H), 7.68 (d, J = 8.3 Hz, 1H), 6.78 (t, J = 5.5 Hz, 1H), 4.88 (s, 2H), 4.35 (s, 2H), 4.35 (t, J = 2.3 Hz, 1H), 4.18 (s, 5H), 3.87 (q, J = 2.3 Hz, 2H), 3.09 (t, J = 2.3 Hz, 1H), 2.94–2.86 (m, 2H), 1.71–1.63 (m, 2H), 1.42–1.22 (m, 4H), 1.35 ppm (s, 9H); ^{13}C NMR ($CDCl_3$, 298 K): δ = 172.08, 170.95, 155.95, 79.40, 78.85, 74.87, 71.37, 70.60, 69.65, 68.41, 68.22, 53.34, 52.62, 40.02, 31.86, 29.37, 28.93, 28.31, 22.70 ppm; MS (ESI+): *m/z* calcd for $C_{25}H_{34}FeN_3O_4$: 496.1899 [M+H^+]; found: 496.1879.

Preparation of Fc-CO-Lys-NH_2 (3): Neat TFA (4 mL) was used to dissolve Fc-CO-Lys-Boc (720 mg, 1.44 mmol). After stirring the solution for one hour, dichloromethane (20 mL) was added to dilute the solution before remove the solvent in vacuum. Three portions of dichloromethane were added and evaporated to get rid of the excess TFA. The residue was dissolved in dichloromethane (10 mL) and TEA (5 mL) was added to convert the TFA salt to free amine completely. After solvent removal, the mixture was used in the next step without further purification.

Preparation of Fc-CO-Lys-ATP (4): Adenosine 5′-triphosphate disodium salt (100 mg, 0.18 mmol) was dissolved in 0.1 M TEAB buffer (pH 7.5) (10 mL) and loaded on a column packed with a cation-exchange resin (AG 50W-X8), which has been pre-equilibrated with 0.1 M TEAB buffer. The desired fraction (monitored by UV light) was collected and evaporated in vacuum. The residue was co-evaporated with dry methanol (10 mL) for three times and dissolved in dry DMF (1.8 mL) under argon. This ATP solution was further dried by pre-activated molecular sieves over night. DCC (123 mg) was added into the ATP solution and the mixture was stirred under Ar for three hours at room temperature to form adenosine-5′-trimetaphosphate (ATMP). The ATMP solution was added to a mixture of compound **3** (8 equiv) in dry MeOH (10 mL) and TEA (0.25 mL, predried by molecular sieves) under Ar. The mixture was stirred for one day, and poured into H_2O (20 mL). The solution was loaded on a DEAE-cellulose column and washed with distilled H_2O to remove excess ferrocene-amine. Then, a linear gradient of TEAB buffer (0.1–0.5 M) was carried out to give the desired fraction (yellow band ≈0.3–0.4 M TEAB), which was lyophilized to give a light yellow powder. The product was further purified by HPLC (Varian

Modular reverse-phase Dynamax Macro-HPLC System C_{18} 21.4 mm × 25 cm). The flow rate was 20 mL min^{-1}, the UV detector was set to $\lambda = 250$ nm, and a 15 min linear gradient was composed of A = TEAB (pH 7.5) and B = CH_3CN from 100 to 95% solvent A for 2 min, from 95 to 80% solvent A for 2 min, from 80 to 75% solvent A for 1 min, at 75% solvent A for 5 min, from 75 to 100% solvent A for 2 min, and at 100% solvent A for 3 min. The product was collected and dried as triethylammonium salt (yield 8%). HPLC: $t_R = 8.3$ min; ^{1}H NMR (D_2O, 298 K): $\delta = 8.42$ (s, 1H), 8.09 (s, 1H), 5.99 (d, $J = 6.0$ Hz, 1H), 4.70–4.63 (m, 3H), 4.44 (t, $J = 2.5$ Hz, 1H), 4.37 (s, 2H), 4.27 (s, 1H), 4.18–4.09 (m, 9H), 3.87 (d, $J = 4.7$ Hz, 2H), 2.78 (q, $J = 7.2$ Hz, 2H), 1.67–1.57 (m, 2H), 1.39–1.01 ppm (m, 4H); ^{31}P NMR (D_2O, 298 K): −0.96 (d, $J = 21.4$ Hz, γ-P), −11.51 (d, $J = 18.3$ Hz, α-P), −23.01 ppm (t, $J = 21.4$ Hz, β-P); MS (MALDI-TOF): *m/z* calcd for $C_{30}H_{40}FeN_8O_{14}P_3$:885.1221 $[M+H]^+$; found: 885.2879.

Substrate cleaning and preparation

All electrochemical experiments were performed by using Au disk electrodes (2 mm diameter, CH Instruments, Inc.). The fluorescence experiments and SECM measurements were performed by using Au silicon sputtering wafers, which were prepared by electron-beam deposition of 200 nm thickness of Au on Si wafer with 20 nm Ti as the adhesion layer (Western University's Nanofabrication Facility). The cleaning of the Au wafers was achieved by etching in piranha solution twenty seconds. After rinsing with Milli-Q water, the Au wafers were further sonicated in Milli-Q water and ethanol for 10 min each, and blown-dried by N_2. The Au electrodes were also cleaned by piranha solution for 2 min. Then 0.3 and 0.05 micron aluminum powder were used for polishing. After rinsing with Milli-Q water and sonication with Milli-Q water and ethanol (10 min each), the electrodes were electrochemically cleaned in 0.5 M KOH by scanning between −2.0 and 0.1 V (vs. Ag/AgCl) at a scan rate of 0.1 V s^{-1} and followed by scanning in 0.5 M H_2SO_4 in the range of 0 to 1.5 V until a stable gold oxidation peak at 1.1 V was obtained.

To immobilize the peptide substrates on the Au wafer and electrode, the Au surface/electrode was first incubated in 2 mM *N*-hydroxysuccinimide lipoic acid active ester (LPA) ethanolic solution at 4 °C for 48 h. Then, the surface was washed with ethanol and incubated with 0.1 mM peptide solution for 24 h at 4 °C. The Au surface was removed from incubation, washed with Milli-Q water thoroughly and further blocked with incubation in 100 mM ethanolic ethanolamine solution for one hour, which was followed with immersion in 10 mM dodecanethiol solution 20 min to back-fill the exposed spots of the surface.

Phosphorylation reaction on the Au surface

The kinase-catalyzed phosphorylation reactions were performed in the kinase assay buffer. The Src kinase assay buffer consisted of 5 mM 3-morpholinopropanesulfonic acid (MOPS) (pH 7.5), 2.5 mM β-glycerophosphate, 1 mM ethylene glycol tetraacetic acid (EGTA), 0.4 mM ethylenediaminetetraacetic acid (EDTA), 2.5 mM $MnCl_2$, and 4 mM $MgCl_2$. The CDK2/cyclin A complex assays were performed in 60 mM 4-(2-hydroxyethyl)-1-piperazineethansulfonic acid (HEPES) (pH 7.5), 3 mM $MnCl_2$, 3 mM $MgCl_2$, 0.05 μg μL^{-1} polyethylene glycol (PEG) 20000 and 3 mM sodium orthovanadate. The CK2α assay buffer consisted of 50 mM Tris HCl (pH 7.5), 10 mM $MgCl_2$, 150 mM NaCl. The peptide-modified surfaces were incubated in the presence of protein kinase (160 ng mL^{-1} for CK2α, and 5 μg mL^{-1} for Src and CDK2) and Fc-CO-C6-ATP or Fc-CO-Lys-ATP or ATP (350 μM). After 8 h of incubation at 37 °C in a heating block (VWR Scientific, USA), the gold substrates were washed by using the kinase assay buffer and then Milli-Q water thoroughly in prior to measurement.

Click reaction on the phosphorylated peptide Au surface

The phosphorylated CK2α peptide-immobilized Au surfaces were prepared according to the same procedure mentioned above. A click-reaction solution containing 0.01% Azide-fluor488, 0.1% CuI, and 1% DIPEA in DMF was applied to the Au surface overnight. Then the Au surface was rinsed thoroughly with DMF, ethanol, and water, and blown-dried with a stream of N_2 in prior to the measurement.

Electrochemical experiments

All electrochemical measurements were carried out by using a CH Instrument potentiostat 660B (Austin, TX). An electrochemical cell with a three-electrode configuration was used with a peptide-modified gold electrode as the working electrode, a platinum wire as the counter electrode, and Ag/AgCl in 3 M KCl as the reference electrode, which was connected by using a salt bridge filled with Agar/3 M KNO_3. The cyclic voltammetry measurements for characterizing the peptide-modified electrodes were performed in 5 mM/5 mM $K_3[Fe(CN)_6]/K_4[Fe(CN)_6]$ solution with 1 M $NaClO_4$ as the supporting electrolyte. Electrochemical impedance spectroscopy (EIS) experiments were conducted in the frequency range of 100 kHz to 0.1 Hz with an AC amplitude of 5 mV. The ZSimpWin 2.0 software (Princeton Applied Research electrochemical software, http://www.princetonappliedresearch.com/Our-Products/Electrochemical-Software/ZSimpWin.aspx) was used to evaluate the EIS data by fitting modeling curves. All impedance spectra are represented as Nyquist plots with real impedance (Z_{re}) and the imaginary impedance (Z_{im}) as the *x* axis and *y* axis, respectively. Square wave voltammetry (SWV) was performed at a pulse amplitude of 25 mV under the same solution condition to EIS. CV and SWV measurements for the phosphorylated peptide-modified electrodes were performed in 1 M $NaClO_4$ as the supporting electrolyte in the potential range of 0.2 to 0.6 V. At least five measurements were performed for all experiments.

Immunoarray fluorescence imaging

After the surface phosphorylation reaction, the Au wafer was immersed in 10% bovine serum albumin (BSA) solution for one hour at room temperature to further eliminate the nonspecific binding of the antibodies. Then the substrates were rinsed in Tris buffer saline Tween20 (TBST) and incubated with a primary Fc-Ab_1 solution (1:500 dilution in 0.1% BSA/TBST) for one hour at room temperature. The Au substrate was then rinsed with TBST and subsequently incubated with secondary antibody (1:100 dilution in 0.1% BSA/TBST) for 45 min at room temperature. The substrates were then rinsed twice with TBST and twice with Tris buffer saline (TBS) and imaged by using a Zeiss AxioPlan2 imaging fluorescent microscope (Zeiss) with filter set 17.

X-ray photoelectron spectroscopy measurement (XPS)

The Au substrates were cleaned and the CDK2 peptide substrate (HHASPRK) was immobilized onto the Au surface by using the same procedure as for the preparation of the modified gold electrode described above. The substrate was subsequently Fc-phosphorylated in the presence of the CDK2/cyclin A complex and Fc-CO-Lys-ATP. Prior to analysis, the substrate was thoroughly rinsed with kinase assay buffer and water, and dried with a stream of N_2.

The XPS analyses were performed with an $Al_{K\alpha}$ X-ray source (15 mA, 14 kV). The operating pressure was 1×10^{-10} Torr. The XPS spectra were obtained with a pass energy of 200 eV for the survey scan and 100 eV for the Fe 2p region. The binding energies were calibrated by using Au $4f_{7/2}$ at 84.0 eV.

Scanning electrochemical microscopy (SECM) measurements

SECM experiments were carried out with a CHI-900b (CH Instruments, Austin, TX) at room temperature in an electrochemical cell by using a three-electrode configuration. A Pt wire, a Ag/AgCl/3.0 M KCl electrode, and a Pt SECM tip were fitted in as the counter electrode, reference electrode, and working electrode, respectively. Modified Au/Si substrates were mounted in the cell and studied during the experiment without bias on the substrates. The homemade Pt tip was fabricated by sealing a Pt wire with a diameter of 25 μm into a glass capillary and then the microelectrode was polished to an RG (ratio of total tip radius to electrode radius) of approximately five. The tip was electrochemically cleaned prior to each experiment by performing cyclic voltammetry scans in 0.5 M H_2SO_4 between 0 and 1.4 V for hundred cycles at a scan rate of 0.5 $V s^{-1}$. The SECM experiments were conducted in the electrolyte, which contains 2 mM $K_4[Fe(CN)_6]$ aqueous solution as the redox probe and 50 mM $NaClO_4$ as the supporting electrolyte. A steady-state current was obtained for each measurement by holding the Pt tip, which was immersed in the electrolyte, at a constant height above the substrate for 300 seconds at a potential of 0.5 V before making the approach. The same potential was applied for making all approach curves measurements. The experimental approach curves were normalized to the steady-state current at an infinite distance before fitting against the theoretical curves simulated by using the COMSOL Multiphysics software.[19b,c] The surface regenerate kinetics was estimated for each set of samples.

Acknowledgements

We are grateful to Rouzbeh Afrasiabi for his help with synthesis. In the initial stage, he helped to synthesize the Fc-CO-Lys-Boc compound. We appreciate funding from NSERCand from the University of Toronto Scarborough.

Keywords: click chemistry · ferrocenes · peptides · phosphorylation · protein kinases

[1] a) G. Burnett, E. P. Kennedy, *J. Biol. Chem.* **1954**, *211*, 969–980; b) G. Manning, D. B. Whyte, R. Martinez, T. Hunter, S. Sudarsanam, *Science* **2002**, *298*, 1912–1934; c) for the use of a Fc-labeled nucleobases by terminal deoxynucleotidyl transferase-mediated 3′-base extension, see: A. Anne, C. Bonnaudat, C. Demaille, K. Wang, *J. Am. Chem. Soc.* **2007**, *129*, 2734–2735.

[2] a) P. Cohen, *Nat. Rev. Drug Discovery* **2002**, *1*, 309–315; b) M. Flajolet, G. He, M. Heiman, A. Lin, A. C. Nairn, P. Greengard, *Proc. Natl. Acad. Sci. USA* **2007**, *104*, 4159–4164.

[3] a) Z. A. Knight, H. Lin, K. M. Shokat, *Nat. Rev. Cancer* **2010**, *10*, 130–137; b) J. Zhang, P. L. Yang, N. S. Gray, *Nat. Rev. Cancer* **2009**, *9*, 28–39; c) M. E. Anderson, L. S. Higgins, H. Schulman, *Nat. Clin. Pract. Cardiovasc. Med.* **2006**, *3*, 437–445.

[4] D. M. Olive, *Expert Rev. Proteomics* **2004**, *1*, 327–341.

[5] a) S. Balakrishnan, N. J. Zondlo, *J. Am. Chem. Soc.* **2006**, *128*, 5590–5591; b) K. Kerman, M. Chikae, S. Yamamura, E. Tamiya, *Anal. Chim. Acta* **2007**, *588*, 26–33; c) K. Kerman, H.-B. Kraatz, *Chem. Commun.* **2007**, 5019–5021.

[6] a) Z. Wang, J. Lee, A. R. Cossins, M. Brust, *Anal. Chem.* **2005**, *77*, 5770–5774; b) Z. Wang, R. Lévy, D. G. Fernig, M. Brust, *J. Am. Chem. Soc.* **2006**, *128*, 2214–2215.

[7] E. T. Lund, R. McKenna, D. B. Evans, S. K. Sharma, W. R. Mathews, *J. Neurochem.* **2001**, *76*, 1221–1232.

[8] Y.-P. Kim, E. Oh, Y.-H. Oh, D. W. Moon, T. G. Lee, H.-S. Kim, *Angew. Chem. Int. Ed.* **2007**, *46*, 6816–6819; *Angew. Chem.* **2007**, *119*, 6940–6943.

[9] a) S. Suwal, M. K. H. Pflum, *Angew. Chem. Int. Ed.* **2010**, *49*, 1627–1630; *Angew. Chem.* **2010**, *122*, 1671–1674; b) K. D. Green, M. K. H. Pflum, *ChemBioChem* **2009**, *10*, 234–237; c) K. D. Green, M. K. H. Pflum, *J. Am. Chem. Soc.* **2007**, *129*, 10–11; d) H. Song, K. Kerman, H.-B. Kraatz, *Chem. Commun.* **2008**, 502–504.

[10] S. Suwal, C. Senevirathne, S. Garre, M. K. H. Pflum, *Bioconjugate Chem.* **2012**, *23*, 2386–2391.

[11] S. Martić, M. Labib, P. O. Shipman, H.-B. Kraatz, *Dalton Trans.* **2011**, *40*, 7264–7290.

[12] a) S. Iijima, F. Mizutani, S. Yabuki, Y. Tanaka, M. Asai, T. Katsura, S. Hosaka, M. Ibonai, *Anal. Chim. Acta* **1993**, *281*, 483–487; b) I. Suzuki, K. Murakami, J.-i. Anzai, *Mater. Sci. Eng., C* **2001**, *17*, 149–154; c) K. A. Mahmoud, H.-B. Kraatz, *J. Inorg. Organomet. Polym. Mater.* **2008**, *18*, 69–80; d) G.-Y. Qing, T.-L. Sun, F. Wang, Y.-B. He, X. Yang, *Eur. J. Org. Chem.* **2009**, 841–849; e) Y. Xiao, M. Petryk, P. M. Diakowski, H.-B. Kraatz, *Proc. SPIE* **2009**, *7304*, 73040R; f) S. Mondal, S. Ghosh, S. Verma, *Tetrahedron Lett.* **2010**, *51*, 856–859; g) M. C. Gimeno, H. Goitia, A. Laguna, M. E. Luque, M. D. Villacampa, C. Sepulveda, M. Meireles, *J. Inorg. Biochem.* **2011**, *105*, 1373–1382; h) M. J. Sheehy, J. F. Gallagher, M. Yamashita, Y. Ida, J. White Colangelo, J. Johnson, R. Orlando, P. T. M. Kenny, *J. Organomet. Chem.* **2004**, *689*, 1511–1520; i) A. J. Corry, A. Goel, P. T. M. Kenny, *Inorg. Chim. Acta* **2012**, *384*, 293–301; j) R. Afrasiabi, H.-B. Kraatz, *Chem. Eur. J.* **2013**, *19*, 15862–15871; k) A. G. Harry, W. E. Butler, J. C. Manton, M. T. Pryce, N. O'Donovan, J. Crown, D. K. Rai, P. T. M. Kenny, *J. Organomet. Chem.* **2014**, *757*, 28–35.

[13] a) T. Hirao, *J. Organomet. Chem.* **2009**, *694*, 806–811; b) T. Moriuchi, T. Nagai, T. Hirao, *Org. Lett.* **2005**, *7*, 5265–5268.

[14] D. R. van Staveren, N. Metzler-Nolte, *Chem. Rev.* **2004**, *104*, 5931–5985.

[15] G. Jaouen, N. Metzler-Nolte, *Topics in Organomet. Chem., Vol. 32*, Springer, Berlin, **2010**, p. 32.

[16] a) S. Martić, M. Labib, D. Freeman, H.-B. Kraatz, *Chem. Eur. J.* **2011**, *17*, 6744–6752; b) S. Martić, M. K. Rains, D. Freeman, H.-B. Kraatz, *Bioconjugate Chem.* **2011**, *22*, 1663–1672.

[17] S. Martić, M. Gabriel, J. P. Turowec, D. W. Litchfield, H.-B. Kraatz, *J. Am. Chem. Soc.* **2012**, *134*, 17036–17045.

[18] H. C. Kolb, M. G. Finn, K. B. Sharpless, *Angew. Chem. Int. Ed.* **2001**, *40*, 2004–2021; *Angew. Chem.* **2001**, *113*, 2056–2075.

[19] a) S. Bergner, P. Vatsyayan, F.-M. Matysik, *Anal. Chim. Acta* **2013**, *775*, 1–13; b) M. N. Alam, M. H. Shamsi, H.-B. Kraatz, *Analyst* **2012**, *137*, 4220–4225; c) P. M. Diakowski, H.-B. Kraatz, *Chem. Commun.* **2009**, 1189–1191; d) J. Kwak, A. J. Bard, *Anal. Chem.* **1989**, *61*, 1221–1227.

[20] R. K. Suto, M. A. Whalen, B. R. Bender, R. G. Finke, *Nucleosides Nucleotides* **1998**, *17*, 1453–1471.

[21] E. Laviron, *J. Electroanal. Chem.* **1979**, *101*, 19–28.

[22] J. Slack-Davis, J. O. DaSilva, S. J. Parsons, *Cancer Cell* **2010**, *17*, 527–529.

[23] D. O. Morgan, *Nature* **1995**, *374*, 131–134.

[24] D. W. Litchfield, *Biochem. J.* **2003**, *369*, 1–15.

[25] P. Y. Bruice, *Organic Chemistry,* 5th ed., Pearson Education, Upper Saddle River, New Jersey, **2007**.

[26] a) Y. Li, R. Afrasiabi, F. Fathi, N. Wang, C. Xiang, R. Love, Z. She, H.-B. Kraatz, *Biosens. Bioelectron.* **2014**, *58*, 193–199; b) S. Martić, M. Labib, H.-B. Kraatz, *Analyst* **2011**, *136*, 107–112.

[27] A. A. Russo, P. D. Jeffrey, A. K. Patten, J. Massague, N. P. Pavletich, *Nature* **1996**, *382*, 325–331.

[28] F. Sicheri, I. Moarefi, J. Kuriyan, *Nature* **1997**, *385*, 602–609.

[29] a) P. Sun, F. O. Laforge, M. V. Mirkin, *Phys. Chem. Chem. Phys.* **2007**, *9*, 802–823; b) J. L. Amphlett, G. Denuault, *J. Phys. Chem. B* **1998**, *102*, 9946–9951; c) M. V. Mirkin, F.-R. F. Fan, A. J. Bard, *J. Electroanal. Chem.* **1992**, *328*, 47–62.

[30] F. Hauquier, J. Ghilane, B. Fabre, P. Hapiot, *J. Am. Chem. Soc.* **2008**, *130*, 2748–2749.

[31] P. M. Diakowski, H.-B. Kraatz, *Chem. Commun.* **2011**, *47*, 1431–1433.

[32] P. C. Reeves, *Organic Syntheses*, Wiley, New York, **2003**.

[33] P. M. Diakowski, Y. Xiao, M. W. P. Petryk, H.-B. Kraatz, *Anal. Chem.* **2010**, *82*, 3191 – 3197.

[34] R. C. Gaussian 03, Revision C. 02 ed., M. J. Frisch, G. W. Trucks, H. B. Schlegel, G. E. Scuseria, M. A. Robb, J. R. Cheeseman, J. A. Montgomery, Jr., T. Vreven, K. N. Kudin, J. C. Burant, J. M. Millam, S. S. Iyengar, J. Tomasi, V. Barone, B. Mennucci, M. Cossi, G. Scalmani, N. Rega, G. A. Petersson, H. Nakatsuji, M. Hada, M. Ehara, K. Toyota, R. Fukuda, J. Hasegawa, M. Ishida, T. Nakajima, Y. Honda, O. Kitao, H. Nakai, M. Klene, X. Li, J. E. Knox, H. P. Hratchian, J. B. Cross, V. Bakken, C. Adamo, J. Jaramillo, R. Gomperts, R. E. Stratmann, O. Yazyev, A. J. Austin, R. Cammi, C. Pomelli, J. W. Ochterski, P. Y. Ayala, K. Morokuma, G. A. Voth, P. Salvador, J. J. Dannenberg, V. G. Zakrzewski, S. Dapprich, A. D. Daniels, M. C. Strain, O. Farkas, D. K. Malick, A. D. Rabuck, K. Raghavachari, J. B. Foresman, J. V. Ortiz, Q. Cui, A. G. Baboul, S. Clifford, J. Cioslowski, B. B. Stefanov, G. Liu, A. Liashenko, P. Piskorz, I. Komaromi, R. L. Martin, D. J. Fox, T. Keith, M. A. Al-Laham, C. Y. Peng, A. Nanayakkara, M. Challacombe, P. M. W. Gill, B. Johnson, W. Chen, M. W. Wong, C. Gonzalez, and J. A. Pople, Gaussian, Inc., Wallingford CT, **2004**.

Received: October 2, 2014
Published online on February 9, 2015